Thomas K. F. Foo, PhD • Anne M. Sawyer, RT[2] • William H. Faulkner, BSRT
Don G. Mills, MD

Inversion in the Steady State: Contrast Optimization and Reduced Imaging Time with Fast Three-dimensional Inversion-Recovery–prepared GRE Pulse Sequences[1]

PURPOSE: **To evaluate the differences in contrast between 1-second delay and zero delay (for magnetization recovery) before the preparation radio-frequency pulse in three-dimensional, inversion-recovery (IR) fast gradient-echo (GRE) acquisitions.**

MATERIALS AND METHODS: **Mathematical simulations and measurements of brain image contrast were performed with healthy volunteers and 10 patients.**

RESULTS: **The zero-delay sequence generated T1-weighted contrast similar to that obtained with 1-second delay but was accompanied by a substantial reduction in imaging time. However, the zero delay prohibits full recovery of the longitudinal magnetization. Hence, the signal null characteristic of IR experiments is not easily observed, since it occurs (as a function of tissue T1) at very short inversion times (<150 msec).**

CONCLUSION: **T1-weighted contrast comparable with that of magnetization-prepared rapid GRE sequences with a 1-second delay and preparation time (TP) of 600–700 msec can be achieved in less time by using a zero delay and a shorter TP (400–500 msec).**

Index terms: Magnetic resonance (MR), contrast enhancement • Magnetic resonance (MR), experimental • Magnetic resonance (MR), fat suppression • Magnetic resonance (MR), k-space • Magnetic resonance (MR), technology

Radiology 1994; 191:85–90

In fast gradient-echo (GRE) imaging techniques, the sequence repetition time (TR) is reduced to between 6 and 18 msec (depending on the image prescription), allowing an image to be acquired in under 2 seconds. To obtain images that are strongly T1 weighted but yet retain the benefits of short image acquisition times, inversion-recovery (IR) radio-frequency (RF) preparatory pulses have been used with fast GRE acquisition segments (1–4). Because the magnetization is sampled during the approach to the steady state after the IR pulse, the k-space acquisition order must be modified to maximize tissue contrast generated by the preparatory pulse (3). However, with all k-space views acquired after a single preparatory pulse, image blurring is an unavoidable consequence of the unequal k-space weighting. Various segmentation schemes have been proposed in which the k space is broken up into different segments, with a preparatory pulse applied for each segment (5,6). However, a delay time after the end of the acquisition of the last view of each segment and before the application of the subsequent preparatory pulse is necessary to allow recovery of the longitudinal magnetization. In two-dimensional image acquisitions, this increase in imaging time with the additional delay period is tolerable, but in three-dimensional volume acquisitions, the time penalty is substantial.

The extension of these initial two-dimensional methods to three-dimensional volume acquisitions has been relatively straightforward. However, owing to long acquisition times, these volume studies have been confined to the evaluation of central nervous system (CNS) disease in which respiratory motion is not a problem. The three-dimensional implementation of the IR-prepared fast GRE acquisition, sometimes referred to as three-dimensional MP-RAGE (for magnetization-prepared rapid GRE), was initially proposed by Mugler and Brookeman (7,8). Initial clinical reports on this technique described the use of a 1–2-second delay for recovery of the longitudinal magnetization (9,10). In addition, these studies (9,10) did not use view reordering to maximize the sensitivity of the data acquisition segments to the IR-prepared magnetization.

Contrast in three-dimensional IR-prepared GRE acquisitions is a function of various parameters. These parameters are the excitation flip angle, sequence TR of the GRE data acquisition segments, inversion time (TI), flip angle of the inversion pulse, and delay time, which permits recovery of the longitudinal magnetization before the IR pulse. Mugler and Brookeman had investigated the optimum white–gray matter contrast achievable with a small 32 × 256 × 128 volume acquisition (8). In that study, they investigated contrast changes as a function of excitation RF flip angles between 0° and 30° and preparation RF pulse flip angles of between 0° and 90°, at a specific (zero) delay time.

Although zero delay (or recovery) times were used in the work by Mugler and Brookeman (8), their study

[1] From the Applied Science Laboratory (T.K.F.F.) and Advanced Applications (A.M.S.), GE Medical Systems, W-975, Box 414, Milwaukee, WI 53201; and Diagnostic Imaging, Chattanooga, Tenn (W.H.F., D.G.M.). From the 1992 RSNA scientific assembly. Received June 8, 1993; revision requested August 9; revision received December 13; accepted December 20. **Address reprint requests to** T.K.F.F.

[2] Current address: Radiological Sciences Laboratory, Lucas Center for MRS/I, Stanford University, Stanford, Calif.

Abbreviations: C/N = contrast-to-noise ratio, CNS = central nervous system, CSF = cerebrospinal fluid, FOV = field of view, GRASS = gradient-recalled acquisition in the steady state, GRE = gradient echo, IR = inversion recovery, RF = radio frequency, SE = spin echo, S/N = signal-to-noise ratio, SPGR = spoiled GRE, TE = echo time, TI = inversion time, TP = preparation time, TR = repetition time.

did not investigate the role of delay times in both optimizing tissue contrast in CNS studies and reducing image acquisition time for a high-resolution volume acquisition suitable for retrospective reformations. An earlier work asserted that the delay time primarily determines the amount of longitudinal magnetization available for measurement and does not affect image contrast (9); however, we hypothesized that the delay time is an important determinant of tissue contrast and that reducing the delay time to zero would reduce the TI and subsequently the total imaging time and yet maintain a similar contrast-to-noise ratio (C/N) and signal-to-noise ratio (S/N). In the study by Brant-Zawadzki et al, the use of a 65-msec delay time was reported (9). However, no comparison was made of the image contrast achieved with short and long delay times.

This article deals specifically with zero-delay-time IR-prepared volume acquisitions. With zero delay times, the (approximately) steady-state longitudinal magnetization is inverted, since there is insufficient time for recovery of the longitudinal magnetization owing to the tissue T1. Subsequently, tissue signal intensities are heavily T1 weighted and are similar to those of conventional T1-weighted spin-echo (SE) images. In marked contrast to IR-prepared volume acquisitions with a 1–2-second delay, the images obtained with zero delay do not exhibit contrast reversals characteristic of IR images. To avoid confusion with conventional IR image contrast, the TI—defined as the interval between the peak of the 180° preparation RF pulse and the peak of the first data acquisition α RF excitation pulse—will subsequently be referred to as a preparation time (TP) rather than a TI. White–gray matter contrast in acquisitions with a zero (minimum) delay time will be compared with that in acquisitions with a 1-second delay time.

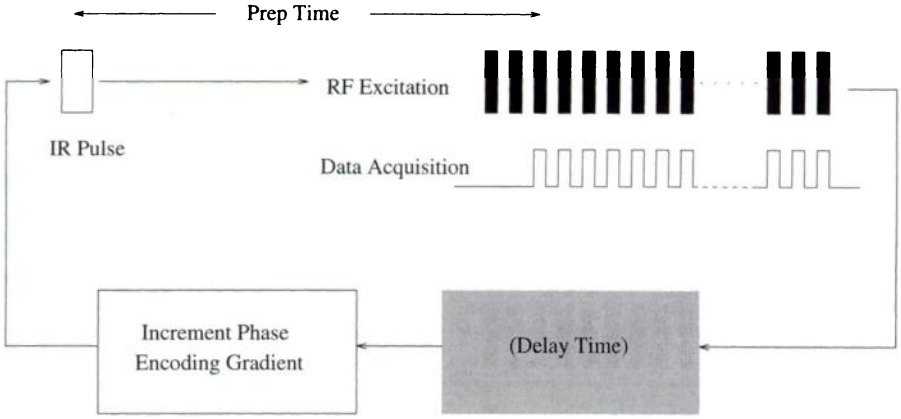

Figure 1. Schematic of the acquisition scheme used in the experiments. Each increment of the phase-encoding gradient lobe is followed by a π preparation pulse and acquisition of all the section-encoding data in a centric order. Note that the TP is measured from the preparation RF pulse to the first RF excitation pulse of the data acquisition segment; any intervening dummy excitations (disdaqs) are ignored. The delay time is the interval after the acquisition of the last section-encoding segment to the subsequent preparation RF pulse. For the minimum/zero-delay acquisitions, this interval is 0 second. Two dummy excitations are shown before data acquisition. *Prep* = preparation.

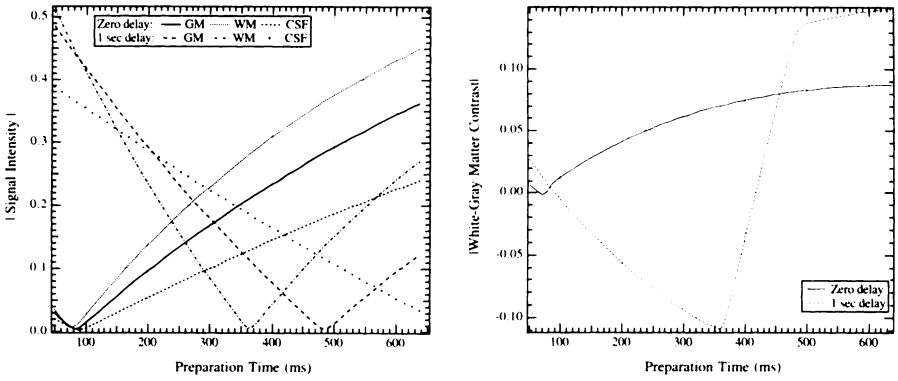

a. b.

Figure 2. **(a)** Theoretical signal intensity curves for gray matter (*GM*), white matter (*WM*), and CSF with 0- and 1-second delay times, as a function of TP. **(b)** Theoretical white–gray matter contrast curves for the 0- and 1-second-delay experiments. The signal intensity and contrast curves for the sequence with a 1-second delay are similar to those of conventional IR acquisitions, while those of the zero-delay sequence are comparable with those of a T1-weighted SE acquisition.

THEORY

The acquisition scheme for an IR-prepared three-dimensional acquisition is shown in Figure 1. In this scheme, all the section-encoding data are acquired after the inversion pulse with a centric acquisition order. The data acquisition segment is typically a fast GRE acquisition in the steady state (GRASS) with partial echo readout to minimize both the echo time (TE) and TR. The data acquisition segment may also be RF phase spoiled (SPGR).

In the subsequent discussion, the section-encoding direction is z, while the directions of the phase-encoding and readout directions are y and x, respectively. After data for the last section-encoding k_z line are acquired, the phase encode gradient lobe is incremented to encode the next k_y line (and k_x–k_z plane data) and the preparation RF pulse is applied immediately without allowing the longitudinal magnetization ($M_{z,eq}$) to recover toward thermal equilibrium (M_0). The sequence is repeated until data for all k-space lines are acquired. For a typical three-dimensional 64 × 256 × 192 acquisition, the magnetization will be approaching the steady state during the acquisition segment. Depending on the tissue T1, excitation flip angle, and TR, the spins may or may not be in the steady state at the end of the acquisition segment. As data are acquired during the approach to the steady state, we can assume that the magnetization at the end of the acquisition segment can be approximated by the steady state expression for an SPGR acquisition, the longitudinal part of which can be written as follows:

$$M_{z,eq} = M_0 \frac{1 - \exp(-TR/T1)}{1 - \exp(-TR/T1)\cos\alpha}, \quad (1)$$

where α is the flip angle of the RF excitation pulse in the data acquisition segment. The expression in Equation (1) was found to be appropriate even for a GRASS acquisition segment, as it takes longer to attain the steady state with a GRASS sequence than with an SPGR sequence. Hence, at the end of the acquisition segment used in the imaging experiments, the longitudinal magnetization for a GRASS readout (in its approach to the steady state) approximates that of the equilibrium M_z value for an SPGR acquisition.

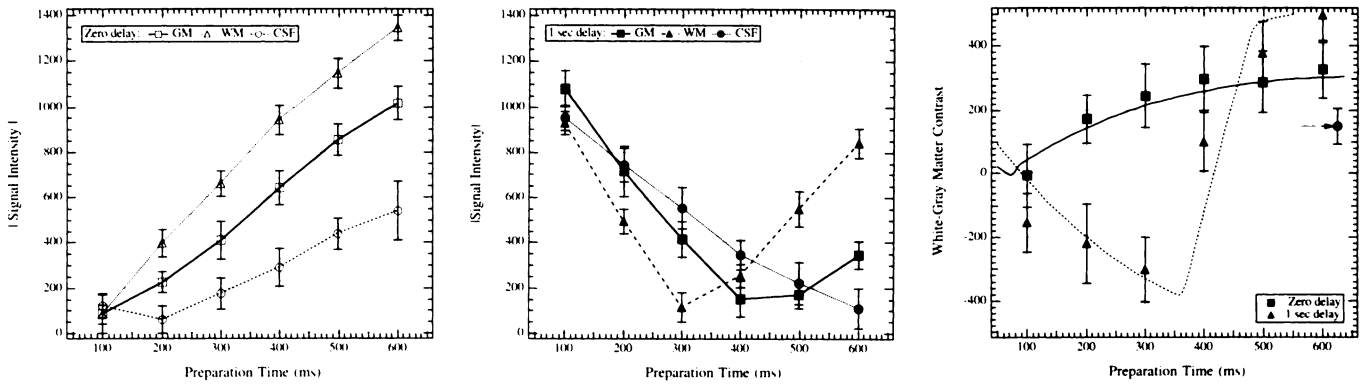

a. b. c.

Figure 3. Experimental signal intensity curves for gray matter (*GM*), white matter (*WM*), and CSF as a function of TP with zero delay time **(a)** and 1-second delay time **(b)**. Signal intensity was measured from magnitude images. **(c)** Experimental white–gray matter contrast curves for the zero- and 1-second-delay experiments. The theoretical contrast curves have been rescaled and plotted on the same graph. The measurements were obtained from images of healthy volunteers. Note the good agreement with the theoretical results. Arrow indicates the measured fast SPGR (20-msec TR, 30° flip angle) contrast for comparison.

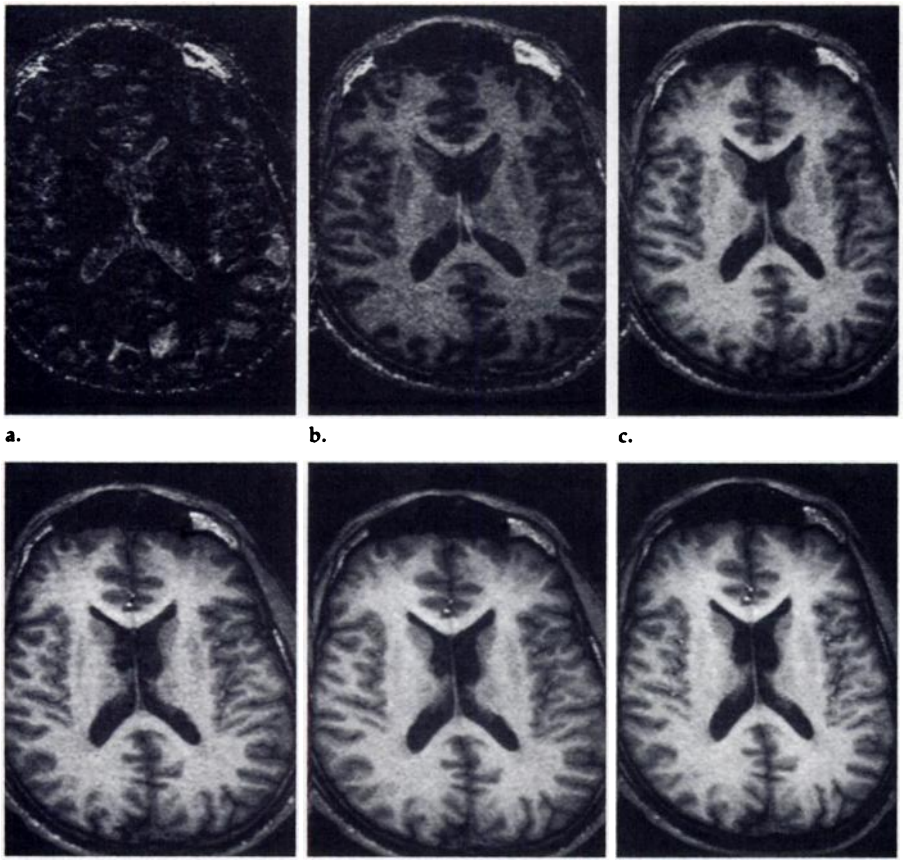

a. b. c.

d. e. f.

Figure 4. Axial images from three-dimensional prepared acquisitions in a healthy volunteer at TPs of 100 **(a)**, 200 **(b)**, 300 **(c)**, 400 **(d)**, 500 **(e)**, and 600 **(f)** msec with zero delay period. Note that the same relative contrast between white and gray matter is maintained with increasing TPs greater than 100 msec. Acquisition parameters were as follows: π preparation RF pulse, 64 × 256 × 192 matrix, 22-cm FOV, 1.5-mm section thickness, 30° flip angle, and TE/TR = 2.3/12.9.

With zero delay times, this value of $M_{z,eq}$ is inverted by the π preparation RF pulse and allowed to recover in time TP before data acquisition. With a 1-second delay period inserted before the π preparation RF pulse, the longitudinal magnetization is allowed to recover toward thermal equilibrium. In addition to creating differences in image contrast, it is obvious that the delay period will prolong the total imaging time by the amount (t_d × *yres*), where t_d is the delay period in seconds measured from the peak of the last RF excitation pulse of the data acquisition segment to the peak of the preparation RF pulse, and *yres* is the in-plane matrix size of the image in the phase-encoding direction.

The maximum available signal after the preparation (π) pulse can be written as

$$M_z = -M_{z,eq}\exp(-t_d/T1) + M_0[1-\exp(-t_d/T1)]\cdot\exp(-TP/T1) + M_0[1-\exp(-TP/T1)], \quad (2)$$

where TP is measured from the inversion pulse to the first α RF pulse of the succeeding data acquisition segment. In practice, two dummy excitations (disdaqs) are applied before data acquisition to minimize blurring of the image point spread function (3). The TP incorporates the time required for the dummy excitations.

MATERIALS AND METHODS

All experiments were conducted on a 1.5-T whole-body Signa MR imaging system (GE Medical Systems, Milwaukee, Wis). A π RF preparation pulse was used in all experiments. Experimental curves for white–gray matter contrast, measured as the signal difference (contrast = $S_a - S_b$), were determined from images of two healthy volunteers. Acquisition parameters used were as follows: 64 × 256 × 192 matrix (number of sections × frequency encodes × phase encodes), 22-cm field of view (FOV), 1.5-mm section thickness, TR msec/TE msec = 2.2/12.9, and 30° flip angle. The measurements were taken with use of a small (20-mm²) region of interest in the caudate nucleus (gray matter), the white matter region immediately adjacent to the caudate nucleus, and the neighboring ventricle (cerebrospinal fluid [CSF]). A GRASS readout acquisition segment was used in all acquisitions.

The section-encoding data were acquired in the innermost loop with a cen-

tric acquisition order. There was no particular reason why the section/view loops could not be interchanged. However, because the number of in-plane phase-encoding views far exceeded the number of section-encoding views, it was preferable to acquire the loop with the shortest total segment acquisition time as the innermost loop. This procedure was performed to maintain as short a readout segment after the preparation pulse as possible to reduce image blurring from unequal weighting of the k-space data. In terms of imaging times, with the same TP, the acquisition with a 1-second delay took almost 3 minutes longer than the acquisition with a zero delay period. Volume acquisitions with RF-phase spoiling but without preparatory pulses were also performed to compare tissue white–gray matter contrast with the prepared acquisitions. In addition to studies of healthy volunteers, 10 patients were also imaged with prepared volume sequences with a TP of 450 msec for the zero-delay acquisition, a TP of 700 msec for the 1-second-delay acquisition, and an RF-phase spoiled volume acquisition without preparatory pulses with a TR of 20 msec.

Another application of a zero-delay prepared technique is to allow the rapid acquisition of volume data with fat suppression. By replacing the spatially selective π preparation pulse with a spectrally selective inversion pulse, fat or water suppression can be attained with short TPs and, consequently, short imaging times. Since the spectrally selective preparation pulse does not affect the unsuppressed spins, the steady state of the unperturbed spins is only mildly interrupted by the preparation RF pulse and the intervening TP and is quickly restored to the steady state during the data acquisition segment. This application required no modification to the pulse sequence except that the preparation RF pulse was replaced with a numerically optimized, spectrally selective π pulse (11).

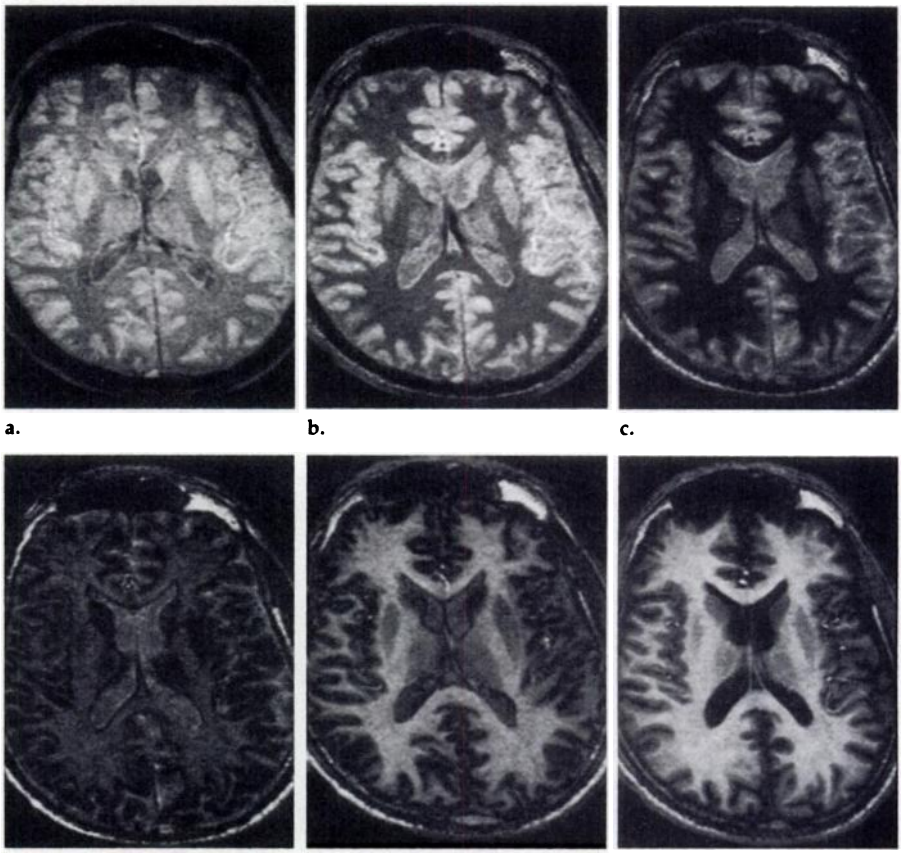

Figure 5. Three-dimensional prepared acquisition in the same volunteer and with the same acquisition parameters as in Figure 4 but with a 1-second delay period. Note the inversion of the white–gray matter contrast at a TP of about 400 msec.

Figure 6. Images in the oblique coronal **(a)** and oblique sagittal **(b)** planes reformatted from a three-dimensional prepared axial acquisition with zero delay at the level of L4-5. The nerve roots are well demonstrated against the thecal sac and epidural fat. The contrast in a zero-delay three-dimensional prepared sequence substantially reduces the signal intensity from long T1 tissues such as CSF, increasing the conspicuity of the nerve roots. Acquisition parameters were as follows: 64 × 256 × 128, two excitations, 22-cm FOV, 2-mm section thickness, 30° flip angle, TE/TR = 5.1/12.4, 500-msec TP. A phased-array coil was used for this volume acquisition, which took 5.6 minutes.

RESULTS

Theoretical signal intensity curves for white matter (T1, T2, and M_0 of 600 msec, 70 msec, and 0.74, respectively), gray matter (920 msec, 85 msec, and 0.80), and CSF (2,000 msec, 1,000 msec, and 1.0) are shown in Figure 2a as a function of TP as in Equations (1) and (2). Figure 2b shows the theoretical white–gray matter contrast curves with zero delay and with a 1-second delay before the preparation RF pulse. The sequence parameters used in these calculations were as follows: 12.9-msec TR, 30° flip angle, and 64 × 256 × 192 acquisition matrix. It is clear from these curves that the image contrast with the 1-second delay is more characteristic of typical IR experiments, in which contrast reversal may occur depending on the TP chosen. The contrast for a zero-delay prepared experiment, on the other hand, is more characteristic of a conventional T1-weighted SE acquisition, in which the same relative contrast is maintained among different T1 species with increasing TPs.

It is also clear that similar tissue signal intensities can be achieved with shorter TPs with zero-delay acquisitions than with 1-second-delay acquisitions. For example, similar signal intensities can be attained with a TP of 400 msec for white matter (with zero delay period), as in an acquisition with a TP of 600–700 msec (with a 1-second delay). However, contrast reversal and signal nulls encountered in the 1-second-delay acquisitions cannot be attained with the zero-delay technique except at extremely short TPs of less than 100 msec. These extremely short TPs are for the most part almost impossible to attain in practice because several dummy RF excitations are required before data acquisition to minimize image blurring.

Measured signal intensity curves, taken as the average of the data from the two healthy volunteers, are shown

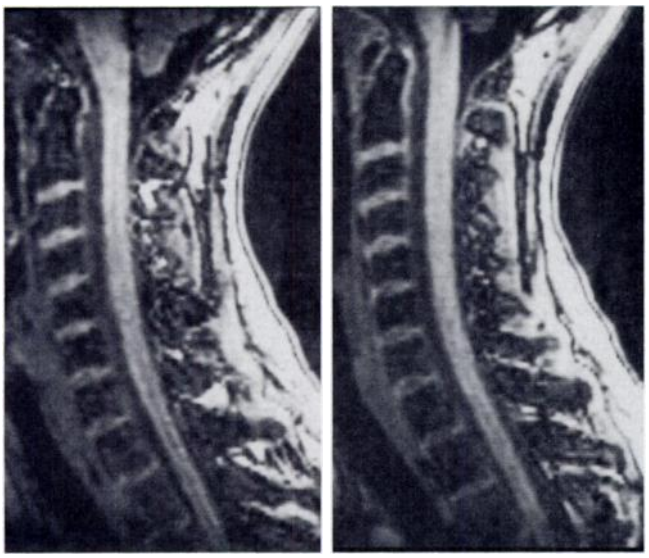

a. b.

Figure 7. Sagittal reformatted images of the cervical spine from an IR-prepared axial volume acquisition with a 400-msec TP. Acquisition parameters were as follows: 128 × 256 × 128 matrix, 20-cm FOV, 1.5-mm section thickness, 30° flip angle, and TE/TR = 2.8/12.5. **(a)** Centric acquisition (imaging time, 3.3 minutes). **(b)** Segmented centric acquisition (imaging time, 5.2 minutes). Increased edge blurring and a slight loss of contrast in the region around the vertebral bodies are evident in **a.**

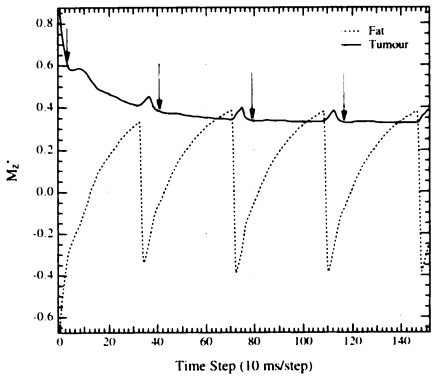

Figure 8. Time history (from Bloch equation simulations) of the longitudinal magnetization for fat and tumor illustrating the effect of a spectrally selective inversion pulse set at the fat resonance. The effect of several inversion pulses and the corresponding TPs are shown. Note that the fat signal is nulled during the acquisition of the low-spatial-frequency views (centric acquisition order), while the magnetization of the nonlipid spins (in this case tumor) is relatively unperturbed. Each time step is a TR segment of 10-msec duration. The arrows indicate the position of the acquisition of the low spatial frequency data in the section-encoding direction.

a. b.

Figure 9. Images of a healthy volunteer, obtained with fat **(a)** and water **(b)** suppression with the same 100-msec TP but with the frequency of the inversion pulse set to the fat and water resonances, respectively. Note the good suppression of fat and water in the respective images. Imaging parameters were as follows: 16-cm FOV, 1.5-mm section thickness, 64 × 256 × 192 matrix, 30° flip angle, and TE/TR = 3.2/11.6. The total imaging time was 2.7 minutes. A prototype phased-array coil was used for this acquisition. Either fat or water suppression was attained in 2.7 minutes for this volume image. In these images, B_0 inhomogeneity resulted in nonuniform suppression, especially in the chest wall.

in Figure 3 together with the measured white–gray matter contrast curves. The results indicate good agreement with the theoretically predicted curves of Figure 2 and imply that the approximation of the longitudinal magnetization at the end of a GRASS readout segment with Equation (1) was valid. Figures 4 and 5 illustrate the change in image contrast at TPs of 100, 200, 300, 400, 500, and 600 msec for the zero-delay and 1-second-delay acquisitions, respectively. As expected, image signal intensity increased as TP was increased for the zero-delay acquisition without a reversal in image contrast. In images acquired with zero delay, tissues with short T1, such as fat or tumors enhanced with gadolinium, return higher signal intensities than do tissues with long T1, such as CSF or gray matter. The images with a 1-second delay exhibited contrast typical of IR-type images, with signal nulls occurring at specific TPs depending on tissue T1. Images with typical T1 weighting (and contrast) were obtained only for TPs greater than 550 msec, whereas the typical T1 weighting was noted at TPs greater than 100 msec with the zero-delay sequence. Although there exists a contrast inversion for the zero-delay sequence, it occurs at such a short TP and with such low image S/N that it ceases to have relevance.

As expected, the white–gray matter contrast for a fast SPGR acquisition without preparatory pulses was less than that attained with either prepared acquisition. However, since the fast SPGR acquisition does not interrogate the magnetization during the approach to the steady state, less image blurring was apparent in the volume reformatted images. The blurring in the prepared acquisition may be reduced by segmenting the data acquisition. For example, the section-encoding data for a k_z of 0 to $+k_{z,max}$ can be acquired after one preparation RF pulse, with the corresponding data for a k_z of 0 to $-k_{z,max}$ acquired after the next preparation RF pulse. Note that the segmentation strategy is feasible for zero-delay acquisitions because it does not substantially increase the total imaging time. How-

ever, if a 1-second delay were to be used, the imaging time would be substantially increased. The contrast obtained in a fast SPGR acquisition with a 20-msec TR and a 30° flip angle is shown in Figure 3 for comparison. With a TR of 20 msec, the total imaging time was approximately equal to that of a zero-delay prepared acquisition with a 400-msec TP and a 12.9-msec TR.

DISCUSSION

Both the theoretical and experimental data indicate that imaging times can be substantially (30%–40%) reduced by using shorter TPs and zero delay times, without compromising image contrast. In fact, image tissue contrast typical of conventional T1-weighted sequences can be obtained in prepared acquisitions with zero delay times. In these images, short T1 species, such as fat or gadolinium-enhanced tumors, exhibited a higher signal intensity than tissues with longer T1 times, such as CSF and gray matter.

The prepared sequence in the steady state has also been determined to be useful in studies of the lumbar spine, where the nerves are well demonstrated against the low signal intensity of the CSF in the thecal sac (Fig 6). Furthermore, the exiting nerve roots are well demonstrated owing to the high contrast difference between the epidural fat and the nerve roots, especially in the volume reformatted images.

In addition to the obvious advantage of reducing the total imaging time below that for prepared images with a 1-second delay time, the prepared acquisition with zero delay permits segmented data acquisition with only a modest increase in total imaging time. This capability is especially useful in volume acquisitions with a large number of sections, such as a 128-section volume acquisition. In this case, the section-encoding views could be segmented so that the positive k-space section-encoding data could be acquired after one IR pulse and the remaining negative k-space data acquired after the succeeding IR pulse (ie, from $k_z = 0$ to $k_z = +k_{z,max}$ and from $k_z = 0$ to $k_z = -k_{z,max}$). This advantage of a segmented acquisition is best appreciated when edges are present in the section-encoding direction, such as in axial acquisitions in the cervical and lumbar spine, in 128-section three-dimensional volumes. Such segmentation has previously been demonstrated to be useful in reducing image blurring due to the nonuniform k-space filter acquiring data during the approach to the steady state in IR-prepared acquisitions (5,6). In the example in Figure 7, some edge blurring was observed at the edges of the cervical spine in the sagittal reformatted images with a single, centric-ordered acquisition segment. Less blurring was observed in the image with the segmented acquisition scheme, although this was attained at the cost of increased imaging time. In this example, the imaging time with segmented acquisition increased from 4.3 to 5.2 minutes.

Fat suppression in a volume acquisition can be attained by using the zero-delay technique and a spectrally selective preparation RF pulse. As shown in the Bloch equation simulation of Figure 8, the fat signal is nulled at a short TP, while the signal from tissue other than fat is relatively unaffected by the preparation RF pulse. This finding allows RF phase spoiling to be used to increase T1 weighting without the accompanying blurring as found in IR-prepared centric acquisitions.

Recall that in the zero-delay acquisition, an extremely short TP tends to suppress signal from almost all spins, especially tissues with long T1 times. By using a spectrally selective preparation RF pulse, either fat or water can be suppressed with the same short TP, without perturbing the steady state of the unsuppressed tissues. As shown in Figure 9, good fat suppression was observed in the breast of a healthy volunteer when the frequency of the inversion pulse was set to the fat resonance with a TP of 100 msec. When the frequency was switched to the water resonance, complete suppression of the nonlipid spins was observed (Fig 9). In both cases, the fat- or water-suppressed volume image with a 64 × 256 × 192 matrix was completed in less than 3 minutes. This technique may be useful in studies of the breast with gadolinium contrast agents. With the fat signal suppressed, the high signal intensity from gadolinium-enhanced tissues (with shortened T1) will not be masked by fat.

In comparison with the prepared acquisitions, as demonstrated in Figure 3c, the fast SPGR volume images exhibited less tissue contrast even when the TR was adjusted for a total imaging time similar to that of the zero-delay acquisition. However, the thrust of this study was to investigate contrast differences between zero-delay and 1-second-delay prepared acquisitions.

There is a distinct advantage in using zero delay times with three-dimensional prepared acquisitions: the reduction in total imaging time without compromised tissue contrast. Fast SPGR acquisition without preparatory pulses offers a steady-state sequence without the pronounced k-space filtering that often occurs in magnetization-prepared acquisitions. In addition, the total imaging time may also be shorter than that for IR-prepared acquisitions, but the reduction in imaging time is accompanied by lower tissue contrast and image S/N. However, various techniques, such as a variable flip angle scheme, can be used to control or minimize the k-space filtering effect (12). ■

References

1. Haase A. Snapshot FLASH MRI: applications to T1, T2, and chemical shift imaging. Magn Reson Med 1990; 13:77–89.
2. Klose U, Nagele T, Grodd W, Petersen D. Variation of contrast between different brain tissues with an MR snapshot technique. Radiology 1990; 176:578–581.
3. Holsinger AE, Riederer SJ. The importance of phase encoding order in ultra-short TR snapshot MR imaging. Magn Reson Med 1990; 16: 481–488.
4. Holsinger-Bampton AE, Riederer SJ, Campeau NG, Ehman RL, Johnson CD. T1-weighted snapshot gradient-echo MR imaging of the abdomen. Radiology 1991; 181:25–32.
5. Chien D, Atkinson DJ, Edelman RR. Strategies to improve contrast in turboFLASH imaging: reordered phase encoding and k-space segmentation. JMRI 1991; 1:63–70.
6. Edelman RR, Wallner B, Singer A, Atkinson DJ, Saini S. Segmented turboFLASH: method for breath-hold MR imaging of the liver with flexible contrast. Radiology 1990; 177:515–521.
7. Mugler JP III, Brookeman JR. Three-dimensional magnetization-prepared rapid gradient-echo imaging (3D MP-RAGE). Magn Reson Med 1990; 15:152–157.
8. Mugler JP III, Brookeman JR. Rapid three-dimensional T1-weighted imaging with the MP-RAGE sequence. JMRI 1991; 1:561–567.
9. Brant-Zawadzki, Gillan GD, Nitz WR. MP-RAGE: a three-dimensional, T1-weighted, gradient-echo sequence—initial experience in the brain. Radiology 1992; 182:769–775.
10. Runge VM, Kirsch JE, Thomas GS, Mugler JP. Clinical comparison of three-dimensional MP-RAGE and FLASH techniques for MR imaging of the head. JMRI 1991; 1:493–500.
11. Foo TKF, LeRoux P, Schneider E. Fat suppression in fast GRASS/SPGR imaging using spectrally selective inversion and saturation RF pulses (abstr). In: Book of abstracts: Society of Magnetic Resonance in Medicine 1992. Berkeley, Calif: Society of Magnetic Resonance in Medicine, 1992; 4403.
12. Mugler JP III, Epstein FH, Brookeman JR. Shaping the signal response during the approach to steady state in three-dimensional magnetization-prepared rapid gradient-echo imaging using variable flip angles. Magn Reson Med 1992; 28:165–185.